

NUMERICAL SIMULATION OF HEAT AND MASS TRANSFER UNDER THE CONDITIONS OF PHASE TRANSITIONS AND CHEMICAL REACTION DURING IGNITION OF CONDENSED SUBSTANCES BY SINGLE HOT PARTICLES

DMITRII O. GLUSHKOV, PAVEL A. STRIZHAK AND
OLGA. V. VYSOKOMORNAYA

National Research Tomsk Polytechnic University
Lenina Avenue, 30, 634050, Tomsk, Russia
E-mail pavelspa@tpu.ru

Key words: Heat and Mass Transfer, Ignition, Condensed Substance, Local Energy Source, Numerical Research.

Abstract. Physical and mathematical models of heat and mass transfer under the conditions of phase transitions and chemical reactions have been developed for the numerical analysis of condensed substances ignition by a single particle (size from 0.5 mm to 5 mm) heated up to high temperature (above 800 K). Liquid, solid and gel fuels were considered as condensed substances. Metal and non-metal particles were used as ignition sources. A heat and mass transfer mathematical model is presented as a system of nonlinear non-stationary differential equations in the private derivatives corresponding to the basic provisions of the general theory of heat transfer in chemical kinetics and free convection. An algorithm for solving differential equations with the corresponding initial and boundary conditions is based on the finite-difference method. The locally one-dimensional method was used to solve difference analogous of differential equations. One-dimensional difference equations were solved using an implicit four-point difference scheme. Nonlinear equations were solved by the iteration method. Mathematical model verification and the assessment of numerical research results reliability was executed by its comparison with experimental results. Also the verification of the law of conservation of energy in the solution area of the ignition problem was performed. Besides, testing of applied numerical methods and the developed silving algorithm on the example of a group of less complex challenges of thermal conduction and thermal convection was held. The minimum parameters of hot particles (temperature, size) and the ignition delay time of condensed substances were determined for local heat sources with different shapes. The influence of thermal conduction, convection and radiative heat transfer mechanisms in the “particle – condensed substance” system was established on the ignition characteristics.

1 INTRODUCTION

The ignition and combustion of various fuels are among the most common technological processes. Their effectiveness is of great importance for the implementation of these processes. Thus, in recent years a large number of theoretical and experimental studies have been devoted to the features and characteristics of heat and mass transfer during local energy supply to various combustible condensed substances (solid, liquid, gel) [1–3]. In particular,

focused light streams, rods heated to high temperatures, hot (with the temperature over 800 K) metal and non-metallic particles may act as local ignition sources. The different mechanisms of heat transfer play a decisive role when using these ignition sources.

It should be noted that among practical applications of the study of condensed substance ignition, there may be identified the technologies of energy efficient fuel initiation, as well as the technologies of fire danger prediction in industries, where the interaction between local heat sources and combustible substances may occur.

The aim of this work is to perform a comparative analysis of the features and characteristics of heat and mass transfer during the ignition of various condensed substances (solid, liquid, gel-like) by single metal and nonmetal particles heated up to high temperatures.

2 PROBLEM STATEMENT

As an example of a numerical model for studying heat and mass transfer during ignition, we consider a model developed for studying the features of these processes during the initiation of gel-like fuel ignition.

The investigation of heat and mass transfer with phase transitions and chemical reactions during the ignition of gel-like condensed substances (hydrazine + 38 % of liquefied oxygen + 5 % of high molecular organic acid salt) has been carried out on the example of the system “hot particle – condensed substance – inert gas” (Figure 1). An oxidizer was thickened by adding salt to render the composition gel state; the temperature of the condensed substance was close to cryogenic (about 90 K). We considered single metal (steel, aluminum) and nonmetal (ceramic, carbon) particles as the sources of limited energy capacity. We examined cylindrical disc shaped particles of small sizes (up to $5 \cdot 10^{-3}$ m) heated up to high (over 1000 K) temperatures.

We considered the following scheme of the investigated process. At the initial time, a hot particle (Figure 1) is deposited inertially on the surface of a cold condensed substance (Figure 1). The subsurface layer of the condensed substance warms up due to the heat generated by the source of limited energy capacity as a result of conductive heat transfer. The additional heat supply in the system (Figure 1) is taken into account during the crystallization of the preheated metal particle material to a temperature above the melting point. Two endothermic phase transitions (melting and evaporation) are implemented consistently in the system “fuel – oxidizer” during the heating of the gel-like condensed substance in the vicinity of the contact border with the hot particle. Fuel and oxidizer vapor enter the area filled with an inert gas due to diffusion-convective mass transfer. The gas-vapor mixture is formed in the vicinity of the energy source. The additional heating of the mixture is transferred from radiation-conductive heat transfer with the hot particle. The temperature growth of the gas-vapor mixture initiates the exothermic interaction between the combustible component (hydrazine) and oxidant (oxygen). One effective chemical reaction is considered to occur. Its speed increases exponentially by the Arrhenius dependence. Gas-phase ignition occurs when the limit (sufficient for ignition) temperatures and concentrations of mixture components are reached. Accepted ignition conditions are similar to the criteria of the gas-phase ignition of liquid condensed substances during local heating [1, 2], which are relevant to the concepts of the modern ignition theory [4]:

1. The energy released as a result of a chemical reaction of fuel oxidation, is more than heat transferred from the heated particle to fuel and the emerging gas mixture.

2. The temperature of the gas-vapor mixture in the localization zone of the leading oxidation reaction exceeds the temperature of the local source of limited energy capacity.

The following assumptions were taken for the model of the investigated process. These assumptions do not impose significant restrictions on the common problem statement:

1. It is not considered the mechanical introduction of the heat source into the subsurface layer of the gel-like condensed substance.

2. It is not considered the burning of the subsurface layer of the gel-like condensed substance.

3. Substances with known thermal and kinetic characteristics are formed during the evaporation of fuel and oxidant. As a rule, the “effective” values of the activation energy E and pre-exponential factor k_0 are determined from experimental studies. These parameters are used for calculating the rate of one “effective” reaction using a first order kinetic scheme.

4. The thermophysical characteristics of substances do not depend on the temperature.

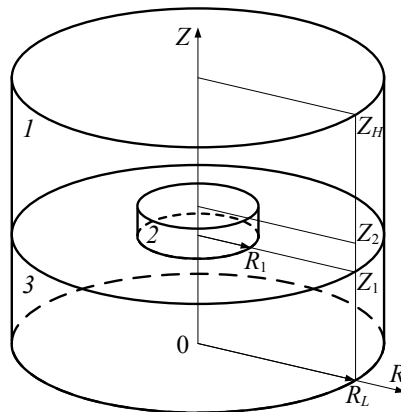


Figure 1: A diagram of the solution area of the ignition problem: 1 – inert gas (gas-vapor mixture), 2 – hot particle, 3 – gel-like condensed substance

Interrelated physical and chemical processes occur during the ignition of the gel-like condensed substance by the local source of limited energy capacity (Figure 1).

3 MATHEMATICAL MODEL AND SOLUTION METHODS

The processes were described by the system of nonlinear nonstationary differential equations of mathematical physics in dimensionless variables. In the mathematical model, we used the elements of numerical algorithms for solving the problems of heat and mass transfer during the ignition of liquid [1, 2] and solid [3] condensed substances by hot particles. This allowed us to obtain a good correlation between theoretical and experimental studies.

Poisson’s equation for gas mixture ($R_1 < R < R_L$, $Z_1 < Z < Z_2$; $0 < R < R_L$, $Z_2 < Z < Z_H$):

$$\frac{\partial^2 \Psi}{\partial R^2} - \frac{1}{R} \frac{\partial \Psi}{\partial R} + \frac{\partial^2 \Psi}{\partial Z^2} = -R\Omega \quad (1)$$

The equation of motion for the gas-vapor mixture:

$$\frac{1}{\text{Sh}} \frac{\partial \Omega}{\partial \tau} + U \frac{\partial \Omega}{\partial R} + V \frac{\partial \Omega}{\partial Z} - U \frac{\Omega}{R} = \frac{1}{\text{Re}_1} \left[\frac{\partial^2 \Omega}{\partial R^2} + \frac{1}{R} \frac{\partial \Omega}{\partial R} + \frac{\partial^2 \Omega}{\partial Z^2} - \frac{\Omega}{R^2} \right] + \frac{\partial \Theta_1}{\partial R} \quad (2)$$

The energy equation for the gas-vapor mixture:

$$\frac{1}{\text{Sh}} \frac{\partial \Theta_1}{\partial \tau} + U \frac{\partial \Theta_1}{\partial R} + V \frac{\partial \Theta_1}{\partial Z} = \frac{1}{\text{Re}_1 \text{Pr}_1} \left[\frac{\partial^2 \Theta_1}{\partial R^2} + \frac{1}{R} \frac{\partial \Theta_1}{\partial R} + \frac{\partial^2 \Theta_1}{\partial Z^2} \right] + \text{Sr}_1 \quad (3)$$

The diffusion equation of fuel vapor in the gas-vapor mixture:

$$\frac{1}{\text{Sh}} \frac{\partial C_f}{\partial \tau} + U \frac{\partial C_f}{\partial R} + V \frac{\partial C_f}{\partial Z} = \frac{1}{\text{Re}_{12} \text{Sc}_{12}} \left[\frac{\partial^2 C_f}{\partial R^2} + \frac{1}{R} \frac{\partial C_f}{\partial R} + \frac{\partial^2 C_f}{\partial Z^2} \right] - \text{Sr}_2 \quad (4)$$

The diffusion equation of oxidant vapor in the gas-vapor mixture:

$$\frac{1}{\text{Sh}} \frac{\partial C_o}{\partial \tau} + U \frac{\partial C_o}{\partial R} + V \frac{\partial C_o}{\partial Z} = \frac{1}{\text{Re}_{13} \text{Sc}_{13}} \left[\frac{\partial^2 C_o}{\partial R^2} + \frac{1}{R} \frac{\partial C_o}{\partial R} + \frac{\partial^2 C_o}{\partial Z^2} \right] - \text{Sr}_2 \quad (5)$$

The balance equation for the gas-vapor mixture:

$$C_f + C_o + C_g = 1 \quad (6)$$

The energy equation for a hot particle ($0 < R < R_1$, $Z_1 < Z < Z_2$):

$$\frac{1}{\text{Fo}_2} \frac{\partial \Theta_2}{\partial \tau} = \frac{\partial^2 \Theta_2}{\partial R^2} + \frac{1}{R} \frac{\partial \Theta_2}{\partial R} + \frac{\partial^2 \Theta_2}{\partial Z^2} + \text{Sr}_3 \quad (7)$$

The energy equation for the gel-like condensed substance ($0 < R < R_L$, $0 < Z < Z_1$):

$$\frac{1}{\text{Fo}_3} \frac{\partial \Theta_3}{\partial \tau} = \frac{\partial^2 \Theta_3}{\partial R^2} + \frac{1}{R} \frac{\partial \Theta_3}{\partial R} + \frac{\partial^2 \Theta_3}{\partial Z^2} - \text{Sr}_4 \quad (8)$$

The numbers of similarity and dimensionless complexes:

$$\text{Sh} = \frac{V_m t_m}{z_H}, \quad \text{Re} = \frac{V_m z_H}{\nu}, \quad \text{Pr} = \frac{\nu C_p}{\lambda}, \quad \text{Sc} = \frac{\nu}{D}, \quad \text{Fo} = \frac{\lambda t_m}{\rho C_p z_H^2}, \quad \text{Sr}_1 = \frac{Q_o W_o z_H}{C_1 \rho_1 \Delta T V_m}, \quad \text{Sr}_2 = \frac{z_H W_o}{\rho_{12} V_m},$$

$$\text{Sr}_3 = \frac{Q_c W_c z_H}{z_p \Delta T \lambda_2} \quad (\text{for the metal particle taking into account material crystallization}), \quad \text{Sr}_3 = 0 \quad (\text{for}$$

$$\text{the nonmetal particle}), \quad \text{Sr}_4 = \frac{Q_m W_m z_H}{z_p \Delta T \lambda_3}.$$

Accepted symbols: τ – dimensionless time; R, Z – dimensionless coordinates of cylindrical system; R_L, Z_H – dimensionless equivalents of r_L, z_H ; z_p – the height of the particle ($z_p = z_2 - z_1$), m; Ψ – dimensionless equivalent of the stream function; Ω – dimensionless equivalent of the vorticity vector; U, V – dimensionless velocity components of fuel vapor in the projection onto the axis R, Z ; Θ – dimensionless temperature; C_f – dimensionless concentration of fuel in the gas-vapor mixture; C_o – dimensionless concentration of an oxidant in the gas-vapor mixture; C_g – dimensionless concentration of an inert gas in the gas-vapor mixture; Sh – Strouhal number; Re – Reynolds number; Pr – Prandtl number; Sc – Schmidt number; Fo – Fourier number; ν – kinematic viscosity coefficient, m^2/s ; ρ – density, kg/m^3 ; C – specific heat capacity, $J/(kg \cdot K)$; λ – thermal conductivity, $W/(m \cdot K)$; D – diffusion coefficient, m^2/s ; Q_m – thermal effect of gel-like condensed substance melting, J/kg ; W_m – mass rate of gel-like condensed substance melting, $kg/(m^2 \cdot s)$; Q_o – thermal effect of fuel vapor oxidation reaction, J/kg ; W_o – mass rate of fuel vapor oxidation, $kg/(m^3 \cdot s)$; Q_c – thermal effect of the crystallization of a metal particle material, J/kg ; W_c – mass rate of the crystallization of the metal particle material, $kg/(m^2 \cdot s)$; indexes: 1 – gas-vapor mixture; 2 – hot particle; 3 – gel-like condensed substance; 12 – fuel vapor; 13 – oxidizer vapor.

The following ratios were used in the transition to dimensionless variables:

$$\tau = \frac{t}{t_m}, R = \frac{r}{r_L}, Z = \frac{z}{z_H}, U = \frac{u}{V_m}, V = \frac{v}{V_m}, \Theta = \frac{T - T_0}{\Delta T}, \Psi = \frac{\psi}{\psi_m}, \Omega = \frac{\omega}{\omega_m},$$

$$V_m = \sqrt{g\gamma\Delta T z_H}, \psi_m = V_m z_H^2, \omega_m = \frac{V_m}{z_H}, \Delta T = T_m - T_0,$$

where t – time, s; t_m – time scale ($t_m = 10^{-3}$ s); r, z – cylindrical system coordinates, m; r_L, z_H – dimensions of the solution area ($r_L = z_H = 0.02$ m); u, v – velocity components of the gas-vapor mixture in projection onto the axis r, z , m/s; V_m – convection velocity scale, m/s; g – acceleration of gravity, m/s^2 ; γ – thermal expansion coefficient, K^{-1} ; T – temperature, K; T_0 – initial temperature of the condensed substance ($T_0 = 90$ K); T_m – temperature scale ($T_m = 1000$ K); ψ – stream function, m^3/s ; ψ_m – stream function scale, m^3/s ; ω – vorticity, s^{-1} ; ω_m – vorticity scale, s^{-1} .

The stream function ψ and a vorticity vector ω :

$$u = \frac{1}{z} \frac{\partial \psi}{\partial z}, v = -\frac{1}{r} \frac{\partial \psi}{\partial r}, \omega = \text{rot}_z \vec{v} = \frac{\partial v}{\partial r} - \frac{\partial u}{\partial z}.$$

The temperature distribution in the solution area of the problem was specified as initial (at $\tau=0$) conditions (Figure 1):

$$\frac{1}{Fo_3} \frac{\partial \Theta_3}{\partial \tau} = \frac{\partial^2 \Theta_3}{\partial R^2} + \frac{1}{R} \frac{\partial \Theta_3}{\partial R} + \frac{\partial^2 \Theta_3}{\partial Z^2} - Sr_4 \quad (8)$$

$$\Theta_1 = \Theta_0, C_f = 0, C_o = 0, \Psi = 0, \Omega = 0 \text{ at } R_1 < R < R_L, Z_1 < Z < Z_2; 0 < R < R_L, Z_2 < Z < Z_H \quad (9)$$

$$\Theta_2 = \Theta_p \text{ at } 0 < R < R_1, Z_1 < Z < Z_2 \quad (10)$$

$$\Theta_3 = \Theta_0 \text{ at } 0 < R < R_L, 0 < Z < Z_1 \quad (11)$$

It was assumed that the thermal contact was ideal at the boundaries “particle – gas”, “particle – condensed substance”, “gas – condensed substance” taking into account the evaporation of fuel and oxidizer vapor from the condensed substance surface and radiant heat removal from the power source surface to surrounding gas environment. The conditions were specified that temperature gradients were equal to zero on the axis of symmetry and the external borders of the solution area.

$$R=0, R=R_L, 0 < Z < Z_1: \quad \frac{\partial \Theta_3}{\partial R} = 0; \quad (12)$$

$$R=0, Z_1 < Z < Z_2: \quad \frac{\partial \Theta_2}{\partial R} = 0; \quad (13)$$

$$R=R_1, Z_1 < Z < Z_2: \quad \frac{\partial \Theta_1}{\partial R} + \frac{q_r}{\lambda_1} \frac{z_H}{\Delta T} = \frac{\lambda_2}{\lambda_1} \frac{\partial \Theta_2}{\partial R}, \Theta_1 = \Theta_2; \quad (14)$$

$$R=0, Z_2 < Z < Z_H;$$

$$R=R_L, Z_1 < Z < Z_H: \quad \frac{\partial \Theta_1}{\partial R} = 0, \Theta_2 = \Theta_1; \quad (15)$$

$$Z=0, 0 < R < R_L: \quad \frac{\partial \Theta_3}{\partial Z} = 0; \quad (16)$$

$$Z=Z_1, 0 < R < R_1: \quad \frac{\partial \Theta_3}{\partial Z} + \frac{z_H}{\lambda_3 \Delta T} (Q_{ef} W_{ef} + Q_{eo} W_{eo}) = \frac{\lambda_2}{\lambda_3} \frac{\partial \Theta_2}{\partial Z}, \Theta_3 = \Theta_2; \quad (17)$$

$$Z=Z_1, R_1 < R < R_L: \quad \frac{\partial \Theta_3}{\partial Z} + \frac{z_H}{\lambda_3 \Delta T} (Q_{ef} W_{ef} + Q_{eo} W_{eo}) = \frac{\lambda_1}{\lambda_3} \frac{\partial \Theta_1}{\partial Z}, \Theta_3 = \Theta_1; \quad (18)$$

$$Z=Z_2, 0 < R < R_1: \quad \frac{\partial \Theta_1}{\partial Z} + \frac{q_r}{\lambda_1} \frac{z_H}{\Delta T} = \frac{\lambda_2}{\lambda_1} \frac{\partial \Theta_2}{\partial Z}, \Theta_1 = \Theta_2; \quad (19)$$

$$Z=Z_H, 0 < R < R_L: \quad \frac{\partial \Theta_1}{\partial Z} = 0. \quad (20)$$

The average thermophysical characteristics of the gel-like condensed substance were calculated by formulas:

$$\lambda_3 = \varphi \lambda_{fs} + (1 - \varphi) \lambda_{os},$$

$$C_3 = \varphi C_{fs} + (1 - \varphi) C_{os},$$

$$\rho_3 = \varphi \rho_{fs} + (1 - \varphi) \rho_{os},$$

where indexes fs – fuel component; os – oxidizer.

The mass rates of the evaporation of fuel and an oxidizer were calculated by the equations:

$$W_{ef} = \varphi \frac{\beta}{1 - k_{\beta}\beta} \frac{(P_e^n - P_e)}{\sqrt{2\pi R_t T_s / M_{12}}},$$

$$W_{eo} = (1 - \varphi) \frac{\beta}{1 - k_{\beta}\beta} \frac{(P_e^n - P_e)}{\sqrt{2\pi R_t T_s / M_{13}}},$$

where β – dimensionless coefficient of evaporation; k_{β} – dimensionless coefficient ($k_{\beta} \approx 0.4$); P_e^n – pressure of saturated fuel vapor (oxidizer), N/m²; P_e – pressure of fuel vapor (oxidizer) near the border of evaporation (calculated according to the Mendeleev–Clapeyron equation), N/m²; R_t – universal gas constant, J/(mol·K); T_s – temperature at the border of phase transition, K; M – molar mass of fuel vapor (oxidizer), kg/kmol.

The mass rate of metal particle material crystallization was calculated by the formula:

$$W_c = V_c \rho_2,$$

where V_c – linear crystallization rate, m/s.

The linear rate of metal particle material crystallization was determined from the following equation:

$$V_c = \frac{\delta(r, z, \tau + \Delta\tau) - \delta(r, z, \tau)}{\Delta\tau},$$

where $\delta(r, z, \tau + \Delta\tau)$ and $\delta(r, z, \tau)$ – the distance between the bottom particle edge and the front of crystallization in the $(\tau + \Delta\tau)$ -th and τ -th time steps, m; $\Delta\tau$ – time step, s.

The mass rate of gel-like condensed substance melting was calculated by the formula:

$$W_m = V_m \rho_3,$$

where V_m – linear melting rate, m/s (calculated similarly to V_c).

The mass rate of fuel vapor oxidation was determined by the Arrhenius equation:

$$W_o = \rho_1 C_f C_o k_0 \exp\left(-\frac{E}{R_t T_1}\right),$$

where k_0 – preexponent of the oxidation reaction, s⁻¹; E – activation energy of the oxidation reaction, J/mol.

The density of heat flux discharged from the heated particle by radiant heat transfer was calculated by the formula:

$$q_r = \sigma \varepsilon T^4,$$

where σ – Stefan-Boltzmann constant, W/(m²·K⁴); ε – emissivity.

The following methods were used for developing the algorithm of the numerical solution of the system of nonlinear nonstationary differential equations with appropriate initial and boundary conditions: finite differences, alternating directions, locally one-dimensional, simple iterations, sweep in the case of an implicit four-point difference scheme.

Recent reports [1–3] described physical and mathematical problems of heat and mass transfer during the ignition of liquid and solid condensed substances by hot particles.

Mathematical modeling was performed with the following parameters [5, 6]: the initial temperature of the gel-like condensed substance and inert gas $\Theta_0=0$, local energy source $\Theta_p=1\div 1.5$; hot particle sizes $R_p=Z_p=0.15$ (Figure 1, $R_p=R_1$, $Z_p=Z_2-Z_1$); the thickness of the condensed substance $Z_1=0.15$; the dimensions of the solution area $R_L=Z_H=1$. The thermal effect of gel-like condensed substance melting $Q_m=395\cdot 10^3$ J/kg, melting temperature $\Theta_m=0.274$. The thermal effects of hydrazine evaporation $Q_{ef}=1390\cdot 10^3$ J/kg and liquefied oxygen $Q_{eo}=2100\cdot 10^3$ J/kg; dimensionless evaporation coefficient $\beta=0.1$; molar mass of fuel vapor $M_{12}=32.05$ kg/kmol and oxidizer $M_{13}=32$ kg/kmol; volume fraction of the fuel component $\varphi=0.57$; kinematic viscosity coefficient of the gas-vapor mixture $\nu=1.41\cdot 10^{-5}$ m²/s; diffusion coefficient of mixture components $D=7.83\cdot 10^{-6}$ m²/s; thermal expansion coefficient $\gamma=0.001$ K⁻¹. The thermal effects of the crystallization of the metallic particle material from steel $Q_c=205\cdot 10^3$ J/kg and aluminum $Q_c=398\cdot 10^3$ J/kg, crystallization temperature $\Theta_c=1.5$ and $\Theta_c=0.95$ respectively. The kinetic parameters of the oxidation reaction of the gas mixture $E=162\cdot 10^3$ J/mol, $k_0=2.25\cdot 10^9$ s⁻¹, $Q_o=14.644\cdot 10^6$ J/kg. The emissivity of steel $\varepsilon=0.55$ and aluminium $\varepsilon=0.06$. The thermophysical characteristics [7, 8] of substances (Figure 1) are shown in Table 1.

Table 1: Thermophysical characteristics

Substance	λ , W/(m·K)	ρ , kg/m ³	C , J/(kg·K)
inert gas	0.026	1.161	1190
hydrazine	0.161	1010	1380
hydrazine vapor	0.072	2.498	3876
liquefied oxygen	0.065	1141	1680
liquefied oxygen vapor	0.027	2.511	2280
steel	49	7831	470
aluminum	98	2700	900
ceramics	20	3800	930
carbon	1.512	1700	1100

Studies [7, 8] described the thermophysical characteristics of liquid (kerosene) and solid metalized fuels.

3 RESULTS AND DISCUSSION

Figure 2 shows the temperature fields at the moment of ignition for three types of condensed substances at local energy supply from a single metal particle. The temperature fields were obtained for liquid and solid condensed substances using the mathematical models developed in studies [1–3]. Previously, it was established that there were three ignition modes typical for the gas-phase ignition of liquid condensed substances when the heat content of a source varied: above the particle (Figure 4a), near its lateral surface, in the immediate vicinity of the border of fuel evaporation. The localization zone of the leading exothermic reaction (Figure 4b) is located in the immediate vicinity of the border of contact with the hot particle near the symmetry axis in the case of the solid-phase ignition of the metalized condensed

substance. Unlike liquid and solid condensed substances, a leading oxidation reaction zone is formed in a small vicinity of the particle base and the boundaries of evaporation products injection (Figure 4c) in the case of the local heating of the gel-like condensed substance subsurface layer by the source of limited energy capacity. It can be seen that an inert gas warmed up substantially faster than fuel and oxidizer components coming from the evaporation surface. The oxidation rate increases when the temperature of the gas-vapor mixture increases due to intensive diffusion-convective heat and mass transfer. Heat release in the system (Figure 1) becomes irreversible, thus ignition occurs.

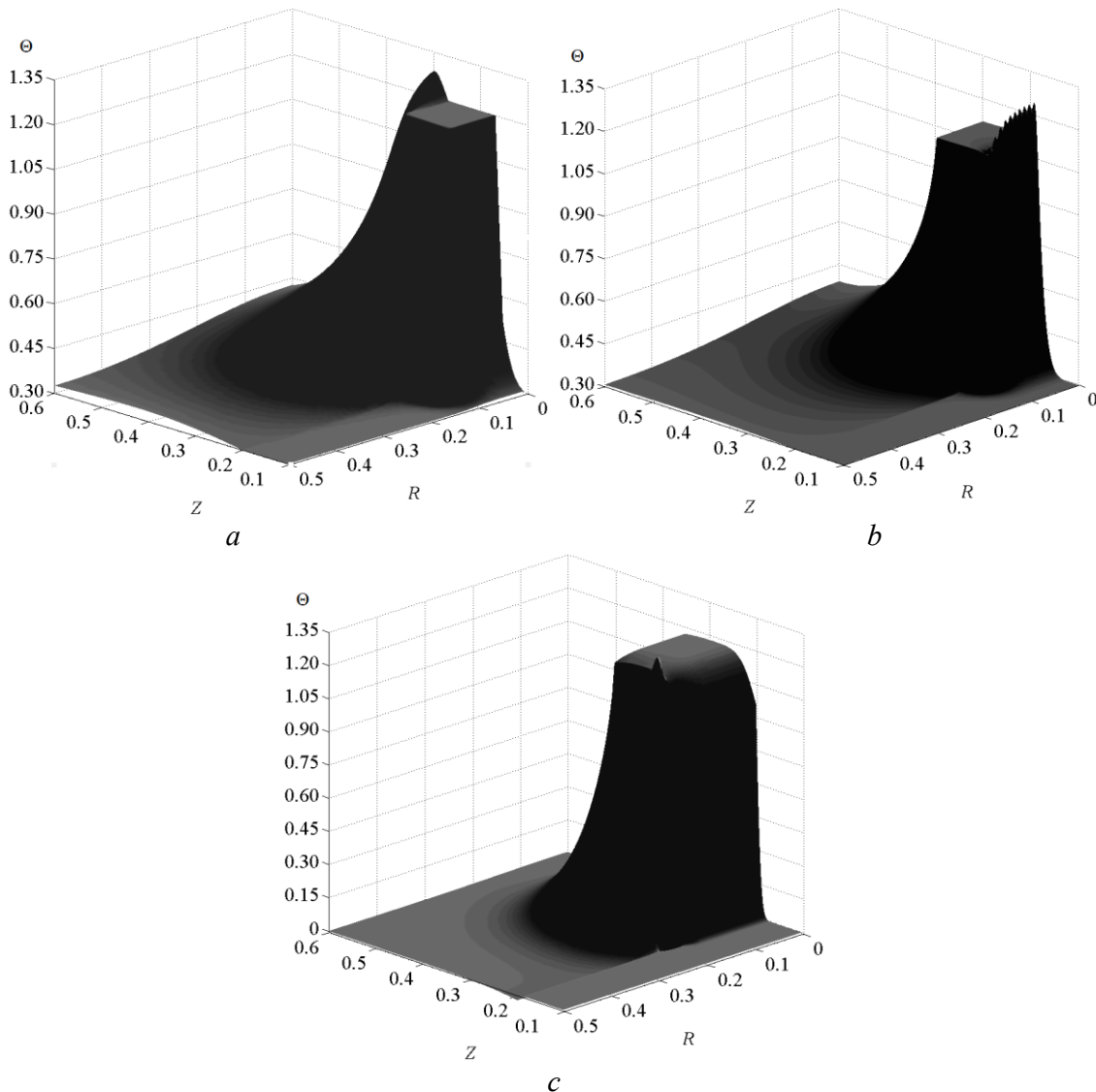


Figure 2: The dimensionless temperature fields at the moment of the ignition of the liquid condensed substance (a) at $R_p=Z_p=0.1$, $\Theta_p=1.2$, metalized solid condensed substance (b) at $R_p=Z_p=0.1$, $\Theta_p=1.2$, gel-like condensed substance (c) at $R_p=Z_p=0.15$, $\Theta_p=1.2$

Table 2 shows the dependencies of dimensionless ignition delay times for liquid, solid and gel-like fuels on the dimensionless initial temperature of the metal particle.

The ignition delay times of the gel-like condensed substance are substantially shorter compared to the similar characteristics of solid and liquid condensed substances. The minimum temperatures of particles ($\Theta_p \approx 1.1$ at $R_p = Z_p = 0.15$, when ignition occurs in the system (Figure 1)), exceed the threshold temperatures of the source ($\Theta_p \approx 1$) to initiate the combustion of solid and liquid condensed substances *ceteris paribus*. Thus, the minimum temperature $\Theta_p = 1.1$ and sizes $R_p = Z_p = 0.15$ of the disc-shaped local source may be assumed as the maximum values for the ignition of the gel-like condensed substance “hydrazine – liquified oxygen”. Established feature can be explained by a significant influence of endothermic phase transitions (melting and evaporation) on the intensity of heat and mass transfer and chemical reaction.

Table 2: Dimensionless ignition delay times τ_d of liquid, solid and gel-like condensed substances depending on the dimensionless initial temperature of a single hot metal particle Θ_p at $R_p = Z_p = 0.15$

Θ_p	1.000	1.100	1.125	1.150	1.175	1.200
Conden- sed substance						
Liquid condensed substance	1.431	1.047	0.923	0.802	0.716	0.604
Solid condensed substance	1.622	0.756	0.627	0.585	0.491	0.464
Gel-like condensed substance	no ignition	0.163	0.108	0.059	0.037	0.028

It should be noted that aluminum, ceramic and carbon particles heated up to high temperatures were used in the experiments as the ignition source. However, the results of numerical studies allowed us to conclude that steel particles had the shortest ignition delay times of condensed substances.

Numerical investigations established the features and differences between the ignition mechanisms of condensed substances during local heating. Thus, it was found that the leading oxidation reaction zone of the gas-vapor mixture is generated around the lateral droplet face in the small vicinity of the contact boundary with the gel-like condensed substance.

The solid condensed substance is characterized by the ignition zone localization near the contact border between fuel and the ignition source. The liquid condensed substance is characterized by three possible localizations: above the particle, near its lateral surface, and in the immediate vicinity of the fuel evaporation border.

Investigations have also revealed the differences between limiting characteristics of the heat source for three types of condensed substances. The temperature limit of the ignition source is $\Theta_p \approx 1$ for liquid and solid condensed substances. The temperature limit of the ignition source is $\Theta_p \approx 1$ for gel-like fuel.

These differences between the main characteristics and features of heat and mass transfer

during the ignition of liquid, solid and gel-like fuels by single hot metal particles, expand modern concepts of the ignition theory [4].

This work was financially supported by the Russian Science Foundation (Project No. 15-19-10003).

REFERENCES

- [1] Kuznetsov, G.V. and Strizhak, P.A. Effect of the Shape of a Particle Heated to a High Temperature on the Gas Phase Ignition of a Liquid Film. *Russ. J. Phys. Chem. B+* (2010) **2**:249–255.
- [2] Kuznetsov, G.V. and Strizhak, P.A. Analysis of Possible Reasons for Macroscopic Differences in the Characteristics of the Ignition of a Model Liquid Fuel by a Local Heat Source and a Massive Heated Body. *Russ. J. Phys. Chem. B+* (2012) **4**:498–510.
- [3] Glushkov, D.O., Kuznetsov, G.V. and Strizhak, P.A. Numerical Study of Ignition of a Metallized Condensed Substance by a Source Embedded into the Subsurface Layer. *Russ. J. Phys. Chem. B+* (2013) **3**:269–275.
- [4] Vilyunov, V.N. and Zarko, V. E. *Ignition of Solids*. Elsevier, Amsterdam, (1989).
- [5] Paushkin, Ya.M. and Chulkov, A.Z. *Rocket fuel*. Moscow, Mir, (1975) [in Russian].
- [6] Sarnet, S. *Chemistry of propellants*. Moscow, Mir, (1969) [in Russian].
- [7] Vargaftik, N.B., Filipov, L. P., Tarzimanov, A. A. and Totkii, E. E. *Handbook of Thermal Conductivity of Liquids and Gases*. CRC Press, Boca Raton, Fla, USA, (1994).
- [8] Vargaftik, N.B. *Tables of Thermophysical Properties of Liquids and Gases*. Hemisphere Publishing, New York, (1975).